Macroscopic equations for pattern formation in mixtures of microtubules and molecular motors

Ha Youn Lee[1] and Mehran Kardar[1,2]
[1]*Department of Physics, Massachusetts Institute of Technology, Cambridge, Massachusetts 02139*
[2]*Institute for Theoretical Physics, University of California, Santa Barbara, California 93106*
(Received 14 February 2001; published 23 October 2001)

Inspired by patterns observed in mixtures of microtubules and molecular motors, we propose continuum equations for the evolution of motor density and microtubule orientation. The chief ingredients are the transport of motors along tubules, and the alignment of tubules in the process. The macroscopic equations lead to aster and vortex patterns in qualitative agreement with experiments. While the early stages of evolution of tubules are similar to coarsening of spins following a quench, the rearrangement of motors leads to arrested coarsening at low densities. Even in one dimension, the equations exhibit a variety of interesting behaviors, such as symmetry breaking, moving fronts, and motor localization.

DOI: 10.1103/PhysRevE.64.056113 PACS number(s): 89.40.+k, 05.70.Fh, 64.60.−i, 05.40.−a

I. INTRODUCTION

The emergence of complex patterns and correlated fluctuations is a characteristic of many out of equilibrium situations [1,2]. Living organisms provide many examples, ranging from the flocking of birds [3,4] and the social organization of bacterial colonies [5–7] to internal reorganization of a cell during division [8,9].

At the molecular level, motors and microtubules are frequently the ingredients responsible for construction and motion. Molecular motors are the proteins that convert chemical energy to mechanical energy, and have been extensively studied [10–12]. Microtubules, consisting of a subunit protein called tubulin, provide the scaffolding for many cell constructs, as well as ''railways'' for transport of proteins [13,14]. In particular, microtubules have a polarity that provides a direction for the transport of motors.

One of the many processes in which motors and microtubules are involved is cell division, during which tubules organize to form a mitotic spindle [8,9]. To elucidate some of the physical mechanisms involved, several *in vitro* experiments on mixtures of microtubules and motors have been carried out [15–17]. Even these simple mixtures result in interesting patterns: At an initial stage the microtubules form an ''aster'' with their ''plus'' ends pointing toward a center. The kinesin based beads move along the microtubules toward this center. In a confined geometry, the aster pattern is then destabilized, giving way to a vortex in which the motors rotate around a center. In unconfined geometries, a variety of self-organized patterns are obtained upon varying the motor concentration. With increasing concentration, an array of vortices, a mixture of asters and vortices, a collection of asters, and bundles of microtubules emerge.

The motivation of this paper is to describe the patterns observed in the *in vitro* experiments. At the outset, it is important to point out that there are fundamental differences between these artificial constructs and the situation in a living cell. First, the experiments use the simplest possible mixture of a single type of motor (kinesin) and microtubules, whereas many more molecules are involved inside a cell. Secondly, to best visualize the patterns, the mixture is confined in *two-dimensional* chambers etched in glass. Finally, Nédélec *et al.* [16] employed an artificial molecular construct consisting of four two-headed kinesin molecules linked by biotin-streptavidin. These motor complexes can attach to two nearby tubules and their motion along the two provides a force that makes them parallel. It is not clear what mechanism operates to align the tubules inside a cell. The experiments, however, have the advantage of simplicity, and can probe the evolution of patterns as a function of a few parameters. The focus of this paper is thus mainly on the artificial situation of mixtures of one type of motor with tubules in two dimensions. Some conjectures about more realistic situations are given at the end.

There are in fact already several models of this system in the literature, starting with the simulations reported in the original paper on the patterns [16]. The microscopic approach of these simulations is well suited for describing the evolution of individual tubules, but is computationally costly for generating large scale patterns. Macroscopic equations which ignore details at short distances are better suited for probing structure at large scales, and can also provide analytical insights. For example, inhomogeneous stripe patterns in two dimensions are predicted by considering a macroscopic field describing tubule orientations [18]. Another recent model introduces a convection-diffusion equation for a motor density field in the presence of a given microtubule array. This model results in a density profile of motors in asters that decays as a power law [19]. In this paper we combine elements from these macroscopic models and consider the coevolution of two continuous fields $m(\vec{r},t)$ and $\vec{T}(\vec{r},t)$, describing the local motor density and tubule orientation, respectively.

Aiming for a minimal description of the observed features, we incorporate only two inputs into the evolution equations for the fields: (i) the motor density is transported along the tubules, while (ii) the tubules are in turn aligned by the motors. We find that simulations of the resulting equations indeed reproduce asters and vortices in agreement with experiment. Analytical solutions of the equations provide further insights into the patterns. For example, we find that the motor density is much larger close to the center of an aster than in a vortex. The resulting increased strain energy

on the tubules provides a driving force for asters to break off to form vortices, in qualitative agreement with experiments. In writing continuum evolution equations for densities, we are following recent studies modeling the flocking of birds [3,4] and the organization of growing bacteria [5–7].

The global evolution of the tubule pattern is sensitive to the initial density of motors. At high density, it is similar to coarsening of XY spins following a quench from high temperatures [20–24]. With periodic boundary conditions, the ultimate pattern is one of aligned tubules, with the motors going around in a uniform current. Such a pattern is not possible with closed boundary conditions, which typically lead to a single vortex in the center. At lower densities, fluctuations play a strong role, and we observe the phenomenon of *arrested coarsening*, in which an inhomogeneous pattern of tubules freezes at some point in time. This occurs because the transport of motors produces regions in which the density of motors is very low (effectively zero). When such regions percolate throughout the system, no further rearrangement of tubules is possible.

To better understand the dynamics of coarsening and sizes of the arrested domains, we also simulated the equations in one dimension. Even in this case, the equations exhibit a variety of interesting patterns that depend on the boundary conditions. (i) With periodic boundary conditions, there is a phase transition between a state with a uniform current of motors running along tubules aligned in one direction (at high motor densities), and one in which there is a localized cluster of motors moving at constant velocity around the system (at low densities). Note that both patterns correspond to a broken symmetry (of the two possible tubule orientations) in one dimension. In contrast to the equilibrium Ising model, this symmetry breaking appears to persist in the presence of noise (mimicking finite temperatures). (ii) Reflecting boundary conditions lead to an oscillating front sweeping back and forth across the system, yet another solitonic solution to the equations. (iii) Closed boundary conditions give rise to initial coarsening and eventual freezing of the tubules into domains. The domain size for frozen tubules depends on the value of the average motor density. Unlike its two-dimensional counterpart, the motor density continues to evolve after the tubules are frozen, and all motors are eventually localized in one cluster.

II. MODEL

Having introduced the local motor density $m(\vec{x},t)$, and the tubule orientation field $\vec{T}(\vec{x},t)$, we would like to explore their evolution in time. There is no simple prescription for devising field equations for nonequilibrium steady states driven by ATP (adenosine triphosphate) hydrolysis. However, symmetries and conservation laws can be used as guides, and provide strong constraints. The conservation of motors leads to the continuity equation

$$\frac{\partial m}{\partial t} = -\vec{\nabla}\cdot\vec{J}_m, \tag{1}$$

where for the motor current we shall assume the form

$$\vec{J}_m = -D\vec{\nabla}m + Am\vec{T} + \cdots. \tag{2}$$

Here, D is the diffusion constant for motors, while A is a coefficient describing their (ATP assisted) transport along the tubule direction $\vec{T}$. We have explicitly included only the lowest order terms in an expansion in powers of m. Higher order terms, such as $Bm^2\vec{T}$ are expected and may become important at high motor densities.

For the evolution of the tubule orientation field $\vec{T}$, we shall employ a similar expansion in small powers, which due to its vectorial character takes the form

$$\frac{\partial \vec{T}}{\partial t} = \alpha\vec{T} - \beta T^2\vec{T} + \kappa\nabla^2\vec{T} + \gamma m\nabla^2\vec{T} + \gamma'\vec{\nabla}m\cdot\vec{\nabla}\vec{T} + \cdots + \vec{f}. \tag{3}$$

The ''local'' terms proportional to α and β describe individual tubules: the linear term gives the tendency for short tubules to grow, while the nonlinear term stops growth of longer tubules mimicking their stabilization by taxol [14]. Dynamical variations in length can be incorporated with a random noise $\vec{f}(\vec{x},t)$. This noise will be mostly ignored in the discussion of patterns, where the initial conditions provide the source of randomness. Neighboring tubule orientations can be coupled through a number of gradient terms. Since in the experiments the alignment of tubules is mediated only by motors, we shall set $\kappa=0$. For simplicity, we also assume that $\gamma=\gamma'$, such that

$$\frac{\partial \vec{T}}{\partial t} = \alpha\vec{T} - \beta T^2\vec{T} + \gamma\vec{\nabla}\cdot(m\vec{\nabla}\vec{T}). \tag{4}$$

The final simplification has the virtue of making the evolution of $\vec{T}$ similar to the familiar minimization of an energy function proportional to $\int[-\alpha T^2/2+\beta T^4/4+\gamma m(\nabla\vec{T})^2/2]$. This is similar to the Landau-Ginzburg energy for vectorial spins, but with a strain energy that is proportional to the local density of motors.

Even the minimal equations involve several parameters. We can bring the equations into simpler form by rescaling to

$$\frac{\partial m}{\partial t} = \nabla^2 m - \vec{\nabla}\cdot(m\vec{T}), \tag{5}$$

$$\frac{\partial \vec{T}}{\partial t} = C\vec{T}(1-T^2) + \vec{\nabla}\cdot(m\vec{\nabla}\vec{T}), \tag{6}$$

where we now measure length in units of $\sqrt{\beta/\alpha}D/A$, time in units of $\beta D/(\alpha A^2)$, motor density in units of D/γ, and the tubule density vector in units of $\sqrt{\alpha/\beta}$. The remaining parameter C is given by $\beta D/A^2$.

III. SIMULATIONS

We perform numerical simulations on a two-dimensional $L\times L$ lattice, adapting the Crank-Nicholson scheme with the alternating direction implicit operator splitting method [25]. The equations are discretized with spatial intervals of

$\Delta x = \Delta y = 1$ and time intervals of $\Delta t = 10^{-2}$. At the edges of a finite system, we employ one of several possible boundary conditions. *Reflecting boundaries* have fixed inward pointing microtubules described by

$$\vec{T}|_{\text{boundary}} = -\hat{n}, \tag{7}$$

where $\hat{n}$ is the normal outward vector at the boundary. This discourages motors from approaching an edge. By contrast, with *parallel boundary conditions* the microtubules are tangential to the boundaries, while *closed boundary conditions* place no restriction on the tubules. In all these cases, there is no current transporting motors outside the system. There is no constraint on the motor current when *periodic boundary conditions* are applied, although again the total number of motors is conserved. The actual boundary condition corresponding to a given experiment will depend on the interaction of the tubules with the confining surfaces. Surface treatments can in principle be applied to favor reflecting or parallel microtubules.

We start with an initial condition in which the motor density is uniformly set to m_0 at all points, while the tubule field has magnitude $|\vec{T}_0| = 10^{-3}$ and random orientations. After a transient period, the homogeneous configuration self-organizes into patterns that depend on the value of average motor density m_0, as well as the growth constant C. Figure 1(a) shows a mixture of vortices and asters which arises as the stationary pattern for $m_0 = 0.01$. Both asters (tubules pointing inward) and vortices (tubules going around) are clearly visible and randomly arranged throughout the system. The motor density now becomes inhomogeneous, with motors accumulating in the centers of vortices and asters [Fig. 1(b)]. The asters are more visible and dominant as the initial motor density increases, as shown for $m_0 = 0.15$ in Fig. 2(a). However, higher densities lead to a single vortex as in Fig. 2(b) for $m_0 = 0.5$ [26].

The dynamics of formation of a large vortex from the random initial conditions is depicted in Fig. 3. This figure corresponds to reflecting boundary conditions, with $C = 10$ and $m_0 = 0.15$. Since the initial tubule length is smaller than unity, the first stages of evolution are the lengthening of tubules as depicted in Figs. 3(a) and 3(b), for times $t = 0.6$ and $t = 1$, respectively. During this stage, the directions of the tubules do not change and they remain randomly distributed. The next stage involves reorientations of the tubules. Since a uniform alignment is incompatible with the boundary conditions, an aster forms in the center as depicted in Fig. 3(c), for $t = 120$. Motors are now transported along the tubules and accumulate at the center of the aster. At longer times, the aster pattern gives way to a vortex as in Fig. 3(d) for $t = 1200$. The vortex pattern is stable, although its center may move around depending on the choice of boundary conditions [26]. This dynamics is consistent with the experimental observation that vortices form from the destabilization of asters [16].

To model pattern formation in larger systems in which boundary effects are less important, we also performed simulations with closed boundary conditions. This change in the boundary condition does not qualitatively alter the pattern

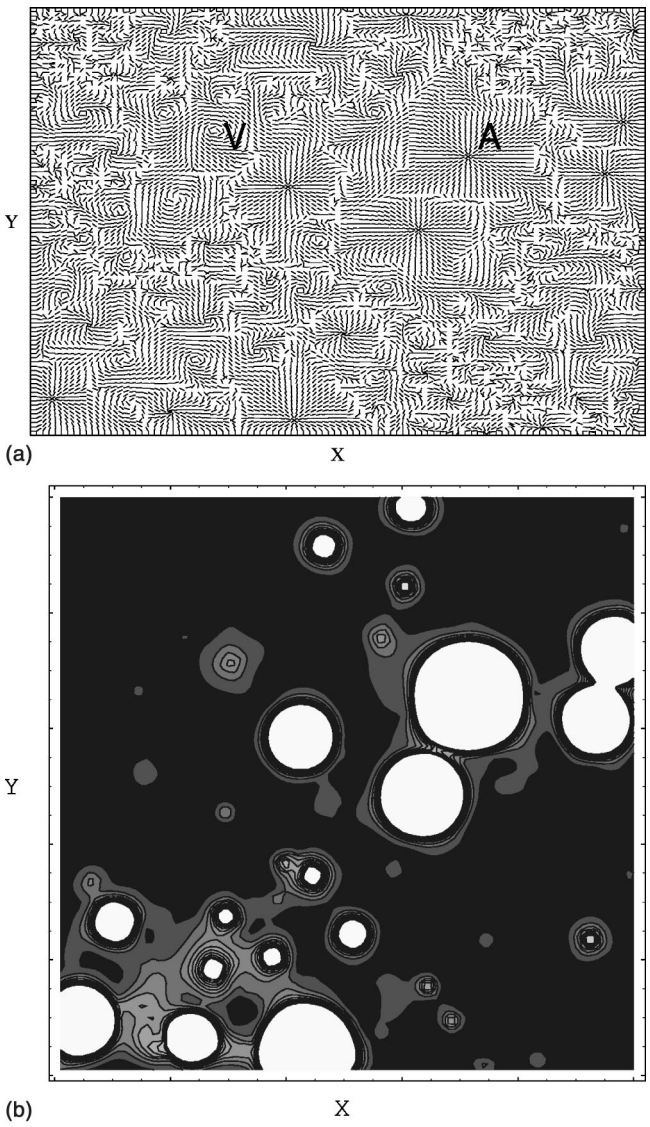

FIG. 1. (a) A collection of vortices and asters for $m_0 = 0.01$ and $C = 100$. The initial size of the tubules is 10^{-3}, while their directions are random. The symbols A and V represent an aster and a vortex, respectively. (b) The corresponding profile of motor density. Gray scale indicates the value of motor density; darker shades indicate smaller values of motor density. The initial homogeneous density evolves to obtain peaks at the centers of asters and vortices.

formation process. At low motor densities, we still observe a mixture of vortices and asters, followed by a collection of asters as m_0 is increased. However, at large motor density, after formation of a large vortex at the center, motors also pile up at several points on the boundary, as indicated in Fig. 4.

Equations (5) and (6) are deterministic, the only stochasticity appearing through the initial conditions. However, randomness and noise are certainly present in the experimental situations. In particular, microtubules are known to constantly grow and shrink though a dynamic instability [13,14], while asters are still observed under such conditions [27]. To make sure that the patterns observed in our simulations survive the addition of noise, we also introduced a stochastic

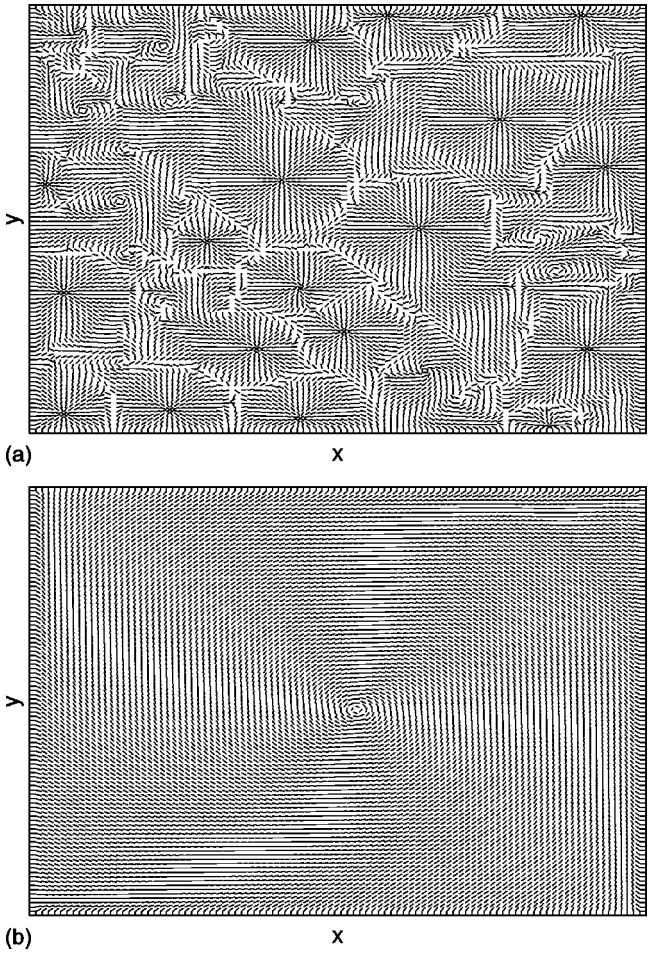

FIG. 2. (a) A collection of asters and vortices for $m_0=0.15$ and $C=100$. The aster patterns become dominant. (b) A large vortex for $m_0=0.5$ and $C=100$. At sufficiently high densities of motors, one or several vortices are formed.

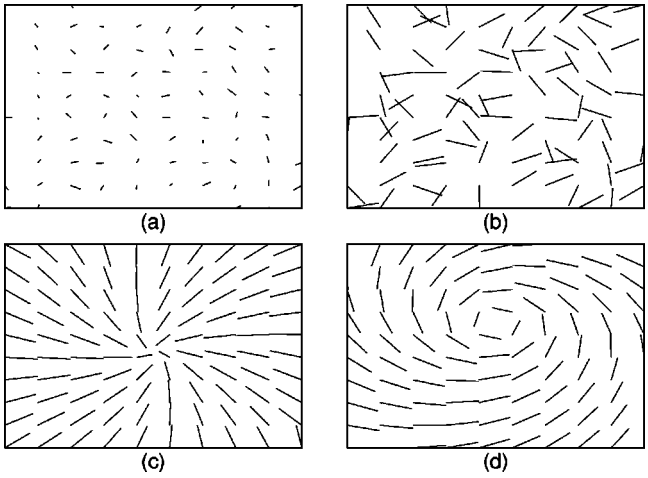

FIG. 3. The evolution of a vortex from an aster at times $t=0.6$ (a), $t=1$ (b), $t=120$ (c), and $t=1200$ (d). The random initial pattern of tubules first grows in length and then organizes as an aster. Motors accumulate at the center of the aster and then circle around when it changes to a vortex.

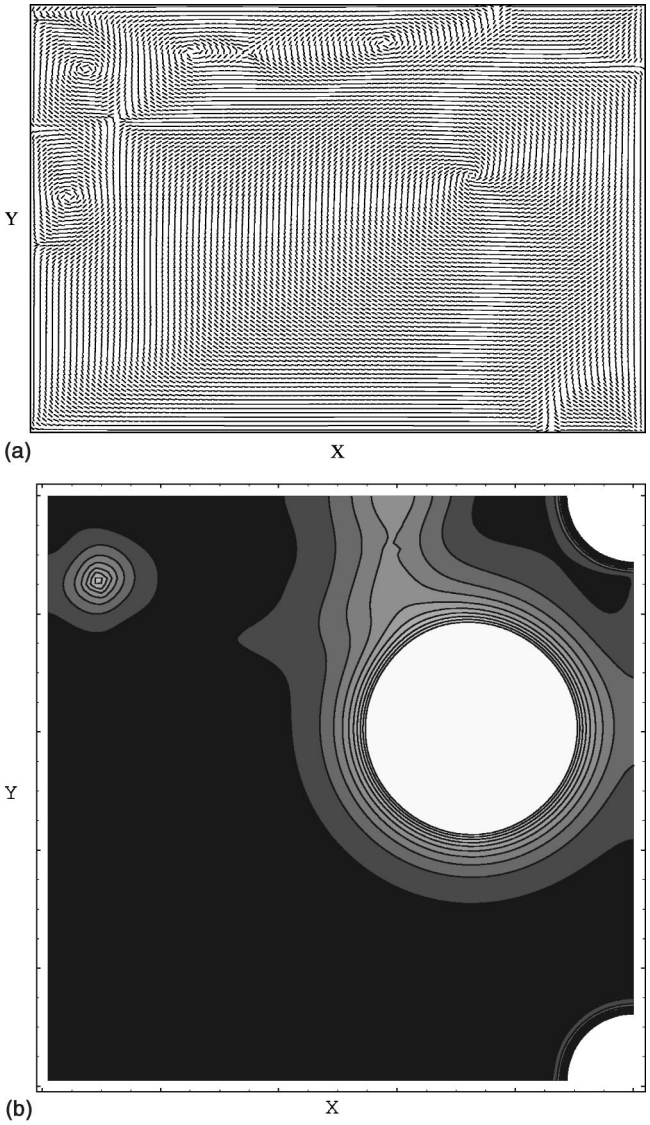

FIG. 4. The configuration of tubules for $m_0=0.5$, with closed boundary conditions (a), and the corresponding profile of motor density (b). Motors pile up at several points on the boundary, in addition to in the interior.

noise in the tubule evolution equation. We observed that the self-organized patterns are stable at small noise, but that sufficiently large noise causes a phase transition to homogeneous mixtures (bundles of microtubules in a uniform motor density). Alternatively, we observe that, for a fixed amount of noise, patterns are destroyed at motor densities lower than a critical m_c, but are qualitatively unchanged otherwise. (The value of m_c is 0.005 if the noise is distributed uniformly between -1 and 1.)

IV. ASTER AND VORTEX SOLUTIONS

We can easily find analytical solutions to Eqs. (5) and (6) that describe the motor density in the center of an aster or vortex. To this end, we look for stationary solutions $\partial_t \vec{m} = \partial_t \vec{T} = \vec{0}$ with radial symmetry. In an aster the tubules are

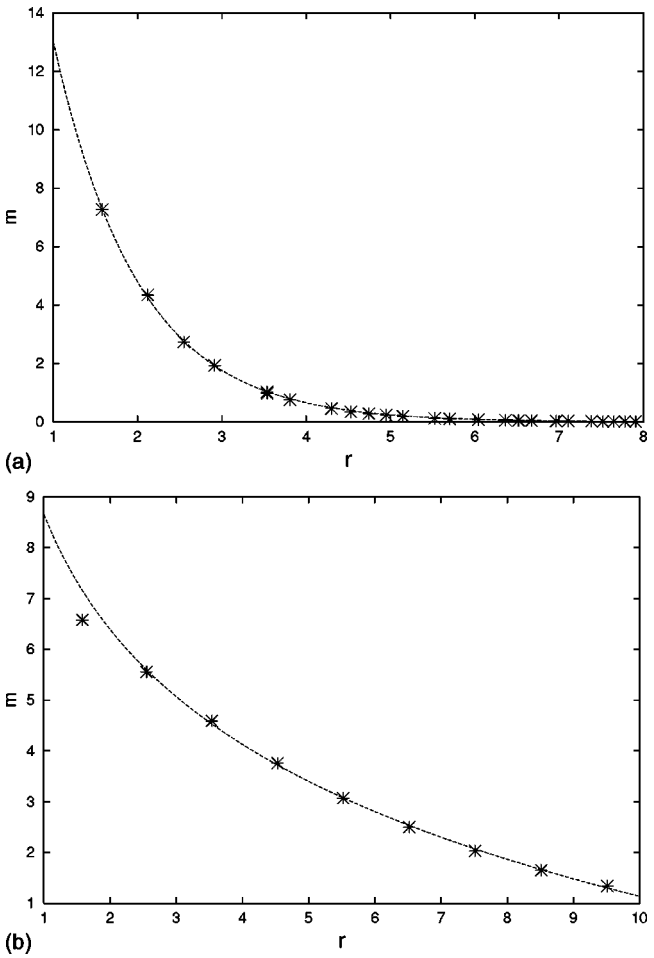

FIG. 5. (a) The points represent the profile of motor density in an *aster* pattern for $m_0=0.1$ and $C=100$. The dashed line is a least-squares fit to the exponential decay $35.4\exp(-r)$. (b) The simulated profile of the motor density of a *vortex* for $m_0=0.2$ and $C=1$. The dashed line is the least-squares fit to the form $-3.3\ln(r/14.2)$.

directed toward the center and $\vec{T}=-\hat{r}$, where $\hat{r}$ is the unit radial vector. Balancing the diffusive current $-\partial_r m$ with that transported along tubules gives an exponential form:

$$m_{\text{aster}}(r)=m(0)\exp(-r). \tag{8}$$

This exponential profile is indeed verified by the simulations as depicted in Fig. 5(a).

The tubules go around the center of a vortex, and $\vec{T}=\hat{\theta}$, where $\hat{\theta}$ indicates the tangential unit vector. Motors are then transported in a uniform circular current by the tubules. To ensure that there is no radial current of motors we need $\partial_r(r\partial_r m)=0$, whose solution is

$$m_{\text{vortex}}(r)=-M\ln(r/R), \tag{9}$$

where R is a long distance cutoff, of the order of the vortex size. A logarithmic fit to the simulated vortex motor density profile is shown in Fig. 5(b).

The profile of motors in quasi-two-dimensional asters has been studied theoretically and experimentally in Ref. [19]. In this study the tubules can grow to form quite long tracks, and their density also falls off away from the aster center. These differences in tubule behavior (as opposed to our case where tubules have uniform density and length) lead to predicted power law decays of the motor density profile.

The aster and vortex configurations of tubules are related to topological defects in the XY model. However, they are equivalent defects in the XY model as one can be deformed into the other through a 90° rotation. The presence and rearrangement of motors in our problem breaks this symmetry and the two configurations become inequivalent. In particular, the two defects have very different static energies $E\propto\int d^2r m(r)(\nabla T)^2/2$. In the aster, the motors are concentrated close to the center leading to a high strain energy. By contrast, the motor density in a vortex is more uniform. Consequently, for the same number of motors, a large aster has much higher energy than a large vortex. Since the dynamics tends to minimize this energy, we have an explanation for why asters give way to the more stable vortices. Presumably, finite size effects in smaller asters, of the order of the decay length implicit in Eq. (8), account for their stability at small motor densities as in Fig. 2(a).

V. ARRESTED COARSENING

If the motor density is maintained at a uniform and fixed value, the dynamics of the tubules is identical to the coarsening of an XY system following a quench from high temperatures. This problem has been extensively studied [20–24] and (up to logarithmic corrections) the typical length scale of the pattern coarsens as $\xi\sim t^{1/2}$. In our case, the motors rearrange themselves in the landscape of the tubules and the coarsening scenario is modified when the motor density fluctuations become significant.

At high motor densities there are enough motors left over after formation of asters and vortices to cause further rearrangements of the tubules, and coarsening continues toward the final pattern consistent with the boundary conditions. However, at low densities the motors quickly migrate to the centers of asters and vortices. The little motor density left in the regions between defects may then be too small to cause further realignment of tubules which became frozen. We call this phenomenon *arrested coarsening* of tubules. The limiting value of m_0 for the onset of arrested coarsening in fact depends on the growth constant of tubules C, as indicated by the tentative ''phase diagram'' sketched in Fig. 6. More simulations are necessary to establish the presence and nature of this transition.

VI. ONE DIMENSION

To further understand the patterns, we examine the equations in one dimension, where more detailed simulations are possible. In particular, we consider scalar fields $m(x,t)$ and $T(x,t)$ evolving as

$$\partial_t m=\partial_x^2 m-\partial_x(Tm), \tag{10}$$

$$\partial_t T=C(T-T^3)+\partial_x(m\partial_x T). \tag{11}$$

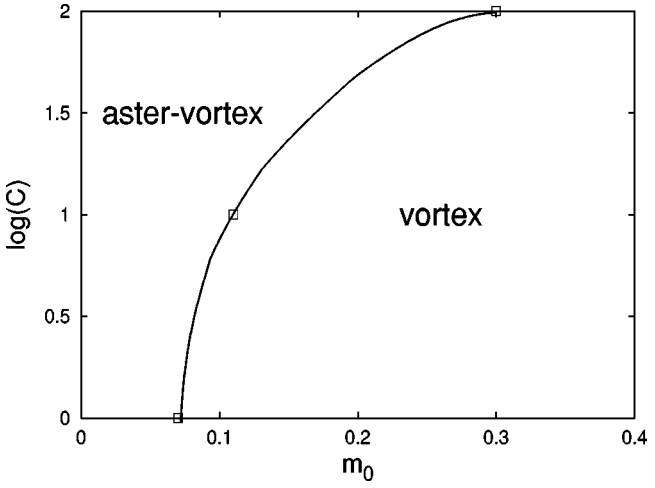

FIG. 6. The phase boundary in the plane of m_0 and $\log_{10} C$. To the right of the boundary the pattern coarsens to a large vortex. The arrested coarsening on the left side leads to frozen asters and vortices, with the aster pattern becoming more dominant as m_0 increases.

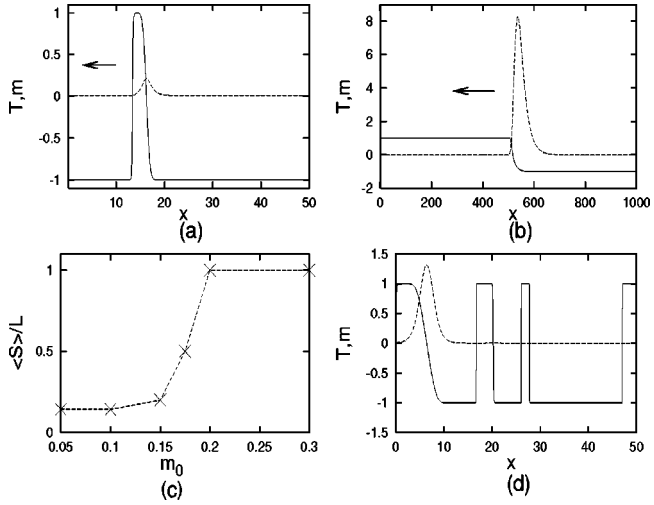

FIG. 7. The profiles of motor density (dashed line) and tubule orientation (solid line) in one dimension with (a) *periodic boundary conditions* for $m_0=0.02$ and $C=1$ and (b) *reflecting boundary conditions* for $m_0=0.4$ and $C=1$. In (a), the whole pattern moves as indicated by the arrow, with a fixed speed. In (b), the cluster of motors moves as indicated by the arrow, but its direction is reversed at each boundary, as the profile oscillates back and forth. (c) The average tubule domain size in a one-dimensional system of length L with closed boundary conditions, as a function of average motor density m_0 for $C=1$. (d) The profiles of tubule orientation and motor density (solid and dashed lines, respectively) for $m_0=0.1$ and $C=1$, in a one-dimensional system with closed boundaries.

Quasi-one-dimensional movement of myosin motors occurs along bundles of actin filaments in muscle contraction, and may also be responsible for other types of cell motion [8]. Bundles of actin molecules can be formed *in vitro* in mixtures with other inert polymers. These bundles consist of random mixtures of actin molecules oriented in the two possible directions. However, in the presence of myosin motors and ATP, there is a sorting of polarity [28,29] and active contraction of polar filaments [30]. To describe such a contraction we need to incorporate additional terms describing the transport of tubules along tubules.

A potential experimental setup for the above equations is a modified version of that used in Ref. [16], with motor/tubule mixtures confined in quasi-one-dimensional channels etched in glass. In addition to periodic channels, it may be possible to model closed and reflecting boundaries by appropriate treatment of the edges. In fact, we observe that the solutions to Eqs. (10) and (11) are quite sensitive to boundary conditions. Specifically, simulations show the following results.

(i) Periodic boundary conditions correspond to placing the system on a closed loop. We observe two types of symmetry breaking depending on the initial density of motors. If m_0 is larger than a critical value of m_c ($m_c \approx 0.04$ for $C=1$), the tubule pattern coarsens until the tubules are all aligned in one direction ($T=+1$ or -1). This is accompanied by a uniform current of motors that goes around the system. This symmetry breaking is similar to that of an Ising model. However, unlike the equilibrium Ising model, here the broken symmetry survives in the presence of random noise (simulating finite temperatures) in Eq. (11). Any domains of opposite spin formed due to randomness are annealed by a rush of motors to the domain walls. The symmetry breaking in the presence of noise is due to the advection term in Eq. (10) and active transportation of motors along the tubules. Indeed we checked that when the advection term is removed, the presence of noise in Eq. (11) leads to finite domains.

If m_0 is smaller than m_c, a final state emerges in which the motors gather together in a cluster that moves around the loop with a constant velocity. The tubules are again ordered in one direction, except near the cluster, where they briefly take the opposite alignment. Figure 7(a) shows the configurations of the tubules and the profile of the motor density for $m_0=0.02<m_c$. We have verified by direct numerical integration that Eqs. (10) and (11) do indeed support such a solitonic solution. However, the mathematical details are not in the spirit of this article, and will be presented elsewhere.

(ii) Reflecting boundary conditions were imposed by requiring the tubules at the edges to point inward, i.e., $[T(0)=+1$ and $T(L)=-1]$. There is an initial coarsening period in which domains of $+1$ and -1 grow inward from the respective edges. However, in the final pattern the boundary between the $+1$ and -1 domains is not stationary, but sweeps back and forth across the system. The motors are again concentrated at the interface, with a solitonic profile as indicated in Fig. 7(b).

(iii) Closed boundary conditions were also applied, with no restrictions on the value of T at the edges, but setting the outward motor current to zero. Above a critical motor density, coarsening of tubules proceeds to a single domain of the size of the system, L. Following the tubules, the motors then pile up at one end of the system. The low density behavior in this case is similar to the arrested coarsening observed in the two-dimensional case: The initial growth of $+1$ and -1 domains is stopped at some point due to the local absence of motors necessary for continuing realignments. Figure 7(c) shows the average domain size, as a function of the average

motor density. At the point when tubule evolution is stopped, the motor density has peaks at $(+,-)$ domain boundaries. However, as time goes on, there is a slower ripening process in which the motors gradually diffuse against the unfavorable domains, and eventually aggregate at one point in the system, as in Fig. 7(d). (It is not clear if this process is truly absent in two dimensions, or merely takes too long to observe in simulations. There are similarities to the localization problem in which 2 is a critical dimension.)

There are similarities in the above behaviors to patterns and phase transitions in other one-dimensional nonequilibrium processes. A localization transition is observed in a population with diffusion, drift, and reproduction in Refs. [31–33]. This model of a bacterial colony living on an oasis in the presence of randomly fluctuating wind shows extended, localized, mixed states, as well as extinction, as a function of the average growth rate and convection velocity. In our model, the tubules (in their disordered state) provide a similar source of random advection. Ordered states are also observed in a lattice model with two species of particles in which the mobility of one species depends on the density of the other [34,35]. This model exhibits three phases: one with strong phase, a fluctuation-dominated phase, and another with uniform overall density. The couplings in our system between motors and tubules have similarities to the latter model, although the enforced conservation laws are different (there is no conservation of tubule orientations).

VII. DISCUSSION

As in the case of driven diffusive systems (see Ref. [36] for a recent review), the rich variety of behavior observed in the relatively simple equations introduced in this paper is due to their nonequilibrium character. In the realm of equilibrium, for example, one-dimensional systems at nonzero temperature are featureless and disordered. Clearly, nonequilibrium effects can lead to symmetry breaking, and a rich interplay of behaviors sensitive to boundaries. Biological systems can take advantage of such phenomena, and should indeed provide many interesting patterns in need of explanation. We conclude by reviewing the successes and failures of our macroscopic modeling of the motor/tubule patterns, pointing out potential extensions and avenues for further exploration.

Given how little input is used to construct the macroscopic equations (tubules transport motors and are aligned in the process), it is encouraging that many features of the experimental patterns are reproduced. As in the experiments, we observe arrays of asters and vortices, and large single vortices (formed from the breakup of asters). A surprising general outcome is the robustness of the patterns to external noise. Many of the large scale features observed (symmetry breaking or large vortices) are easily destroyed in equilibrium by thermal noise, but are maintained in the nonequilibrium steady states.

The limitations of the model are also due to the limited input. For example, at high densities of motors the experiments lead to irregularly arranged bundles of tubules; a feature not present in our model. To reproduce the observed sequence of patterns, more physical input into the equations is necessary. A potential modification is to impose a saturation on the ability of motors to align tubules at high motor densities. Indeed, such saturation generates an irregular pattern of tubules, instead of a large vortex, at high motor densities.

A simple yet relevant extension of our model is to consider mixtures of tubules with two types of motor, kinesin and dyenin, which are transported in opposite directions [37]. Preliminary simulations indicate various patterns such as asters, antiasters, and vortices, but a global phase diagram has not yet been constructed. Another interesting extension is to examine the patterns predicted by the model in three dimensions; corresponding simulations are straightforward, albeit more time consuming.

Independent of their relevance to the motor/tubule system, the equations presented in this paper exhibit a variety of interesting behavior worthy of further investigation. From the perspective of statistical mechanics it is interesting to rigorously characterize the distinct phases encountered, and the nature of the transitions between them. The symmetry breakings in one dimension are particularly interesting as they do not have equilibrium counterparts. The solitonic solutions to these equations can be further explored by standard mathematical methods. Finally, with a view to describing the contraction of muscle fibers, the addition of drift terms to the equation for tubules is desirable.

ACKNOWLEDGMENTS

We wish to thank F. J. Nèdèlec and P. De Wulf for helpful discussions. H.Y.L. is supported by the Korea Science and Engineering Foundation. M.K. acknowledges the support of NSF Grants No. DMR-98-05833 (at MIT) and No. PHY99-07949 (at ITP).

[1] M. C. Cross and P. C. Hohenberg, Rev. Mod. Phys. **65**, 851 (1993).
[2] J. P. Gollub and J. S. Langer, Rev. Mod. Phys. **71**, S396 (1999).
[3] T. Vicsek, A. Czirok, E. Ben-Jacob, I. Cohen, and O. Shochet, Phys. Rev. Lett. **75**, 1226 (1995).
[4] J. Toner and Y. Tu, Phys. Rev. Lett. **75**, 4326 (1995).
[5] H. C. Berg, Nature (London) **254**, 389 (1975).
[6] E. O. Budrene and H. C. Berg, Nature (London) **349**, 630 (1991).
[7] E. Ben-Jacob, I. Cohen, O. Shochet, A. Tenenbaum, A. Czirok, and T. Vicsek, Phys. Rev. Lett. **75**, 2899 (1995).
[8] B. Alberts *et al.*, *The Molecular Biology of the Cell* (Garland, New York, 1994).
[9] A. Hyman and E. Karsenti, Cell **45**, 329 (1986).
[10] K. Svoboda, P. P. Mitra, and S. M. Block, Proc. Natl. Acad.

Sci. U.S.A. **91**, 11 782 (1994).
[11] K. Visscher, M. J. Schnitzer, and S. M. Block, Nature (London) **400**, 184 (1999).
[12] M. E. Fisher and A. B. Kolomeisky, Physica A **274**, 241 (1999).
[13] T. Mitchison and M. W. Kirschner, Nature (London) **312**, 237 (1984); **312**, 232 (1984).
[14] M. Dogterom and S. Leibler, Phys. Rev. Lett. **70**, 1347 (1993).
[15] R. Urrutia *et al.*, Proc. Natl. Acad. Sci. U.S.A. **88**, 6701 (1991).
[16] F. J. Nédélec, T. Surrey, A. C. Maggs, and S. Leibler, Nature (London) **389**, 305 (1997).
[17] T. Surrey *et al.*, Proc. Natl. Acad. Sci. U.S.A. **95**, 4293 (1998).
[18] B. Bassetti, M. C. Lagomarsino, and P. Jona, Eur. Phys. J. B **15**, 483 (2000).
[19] F. Nédélec, T. Surrey, and A. Maggs, Phys. Rev. Lett. **86** 3192 (2001).
[20] M. Mondello and N. Goldenfeld, Phys. Rev. A **42**, 5865 (1990).
[21] A. N. Pargellis, S. Green, and B. Yurke, Phys. Rev. E **49**, 4250 (1994).
[22] A. J. Bray and A. D. Rutenberg, Phys. Rev. E **49**, R27 (1994).
[23] A. D. Rutenberg and A. J. Bray, Phys. Rev. E **51**, R1641 (1995).
[24] F. Rojas and A. D. Rutenberg, Phys. Rev. E **60**, 212 (1999).
[25] W. H. Press, B. P. Flannery, S. A. Teukolsky, and W. T. Vetterling, *Numerical Recipes in C* (Cambridge University Press, Cambridge, 1988).
[26] With boundary conditions of inward pointing tubules, the center of the single vortex moves around the center of the system. However, with tubules aligned parallel to the boundary, the pattern of the final vortex is stationary.
[27] T. Mitchison and M. Kirshcner, Nature (London) **312**, 232 (1984).
[28] K. Takiguchi, J. Biochem. (Tokyo) **109**, 520 (1991).
[29] H. Nakazawa and K. Sekimoto, J. Phys. Soc. Jpn. **65**, 2404 (1996).
[30] K. Kruse and F. Jülicher, Phys. Rev. Lett. **85**, 1778 (2000).
[31] D. R. Nelson and N. M. Shnerb, Phys. Rev. E **58**, 1383 (1998).
[32] K. A. Dahmen, D. R. Nelson, and N. M. Schnerb, J. Math. Biol. **41**, 1 (2000).
[33] K. A. Dahmen, D. R. Nelson, and N. M. Schnerb, e-print cond-mat/9903276.
[34] D. Das and M. Barma, Phys. Rev. Lett. **85**, 1602 (2000).
[35] S. Ramaswamy, M. Barma, D. Das, and A. Basu (unpublished).
[36] B. Schmittmann and R. K. P. Zia, in *Proceedings of the IXth International Summer School on Fundamental Problems in Statistical Mechanics*, edited by H. van Beijeren [Phys. Rep. **301**, 45 (1998)].
[37] T. Surrey *et al.*, Science **292**, 1167 (2001).